RSC Advances

PAPER

View Article Online
View Journal | View Issue

Cite this: *RSC Adv.*, 2023, **13**, 35639

The enzymatic synthesis of lactose caprate using *Candida rugosa* lipase immobilized into ZIF-8 and investigation of its anticancer applications against K562 leukemia and HeLa cancer cells†

Effat Karimian,[a] Afsaneh Marandi,[a] Reihaneh Kardanpour,[a] Sara Rafiei,[a] Zahra Amirghofran,[b] Shahram Tangestaninejad,*[a] Majid Moghadam,*[a] Valiollah Mirkhani[a] and Iraj Mohammadpoor-Baltork[a]

In this study, a lactose fatty acid ester was enzymatically synthesised using immobilized *Candida rugosa* lipase (CRL). Its anticancer property against K562 leukemia and HeLa cancer cells was carefully investigated. In the first step, a *de novo* strategy was applied to encapsulate CRL into a microporous zeolite imidazolate framework called ZIF-8. Various characterization techniques including powder X-ray diffraction, Fourier transform infrared spectroscopy, N_2 adsorption–desorption, field-emission scanning electron microscopy and thermogravimetric analysis were used to prove the successful encapsulation of CRL molecules during the formation of ZIF-8 crystals with an enzyme loading of 98% of initial CRL. The effect of various factors such as pH and temperature, affecting the enzymatic activity and reusability of the CRL@ZIF-8 composite were assessed against the free enzyme. Additionally, enzyme catalysis parameters, such as K_m and V_{max}, were also assessed. The obtained biocatalyst showed excellent activity in a wide pH range of 2–9 and a temperature range of 30–60 °C. According to the experimental results, the CRL@ZIF-8 composite maintained about 63% of its initial activity after 6 cycles of use. In the next step, the synthesized catalyst was applied for the synthesis of lactose caprate *via* enzymatic esterification of lactose with capric acid. Further experiments were performed to obtain the cytotoxicity profile of the new derivative. The growth inhibitory effect of the produced lactose caprate on K562 leukemia and HeLa cancer cells determined by the MTT (3-(4,5-dimethylthiazol-2-yl)-2,5-diphenyltetrazolium bromide) assay showed its potential anticancer effects against both cell lines (IC_{50}, 49.6 and 57.2 μg mL^{-1}). Our results indicate that lactose caprate might be a promising candidate for further studies on K562 leukemia and HeLa cancer cells owing to its possible therapeutic usefulness.

Received 11th July 2023
Accepted 23rd October 2023

DOI: 10.1039/d3ra04632j

rsc.li/rsc-advances

1 Introduction

The esterification of sugars with fatty acids produces sugar fatty acid esters (SFAEs), which are popular food additives. Sugar fatty acid esters are non-toxic, biodegradable and biocompatible non-ionic surfactants and possess a wide range of hydrophilic–lipophilic balance values.[1] Therefore, they have supplemental advantages, such as anti-cancer, antibacterial and insecticidal properties, over conventional surfactants, which render them ideal for synthetic surfactants in cosmetic, food and pharmaceutical industries as well as for biomedical applications.[2–4]

Despite the growing interest for the synthesis of sugar esters from different sugars, such as glucose, fructose and maltose, very few studies have been reported on lactose.[1,5–7] Lactose is a disaccharide and the main sugar in whey and milk, which can be transformed into value-added products, such as biosurfactants, alcoholic beverages and lactic acid.[8] Lactose monoester derivatives were synthesized in the 1970s for the first time and received increasing attention due to their potential anticancer activity.[9,10] Capric acid, the main constituent of goat milk, was our choice of a saturated fatty acid owing to its inhibitory effect on different cancer cells, especially on colon and skin cancers.[11] The esterification of capric acid and lactose produces an amphiphilic product that can modify the bioavailability of drugs and augment the absorption of macromolecular drug across the epithelia.[12,13]

Among the chemical and enzymatic methods for the synthesis of SFAEs, the latter methodology is a more preferable approach, which is notably more chemo- and regio-selective,

[a]*Department of Chemistry, Catalysis Division, University of Isfahan, Isfahan 81746-73441, Iran. E-mail: stanges@sci.ui.ac.ir; moghadamm@sci.ui.ac.ir*

[b]*Immunology Department, Autoimmune Diseases Research Centre, Shiraz University of Medical Sciences, Shiraz, Iran*

† Electronic supplementary information (ESI) available. See DOI: https://doi.org/10.1039/d3ra04632j

capable of producing purer products and is more environment friendly.[2,14] According to the previously reported studies, it seems that the lipase enzyme can be an excellent option for the SFAE production. Lipase can catalyze a wide variety of novel chemical reactions, such as esterification, transesterification and synthesis of peptides and other chemicals, in both aqueous and non-aqueous media.[15] *Candida rugosa* lipase (CRL) is a versatile and prominent biocatalyst owing to its notable properties such as high activity, excellent stability and substrate specificity.[16] On the flip side, the lipase enzyme is not economically viable, and if applied as a free catalyst, it cannot be recovered from the reaction media and may contaminate the final product. Therefore, the immobilization of enzymes using solid supports is not only crucial from the economic standpoint but also important for improving the enzyme efficiency, stability, and recyclability.[17] Till date, the cross-linking of lipase and its covalent attachment to the amino-functionalized support has been well studied. Zaidan *et al.* reported the biocatalytic properties of mica-based immobilized lipases and evaluated the effect of fatty acid chain length and different important parameters in the SFASE syntheses.[18]

Metal–organic frameworks (MOFs) are highly tunable and porous materials with a vast range of applications that meet requirements as the best candidates for enzyme immobilization due to their versatile functional group.[19,20] Among the different strategies for enzyme immobilization including surface adsorption, surface immobilization, and encapsulation, the last method is considered the best strategy. Nevertheless, the large dimension of most enzymes compared to the small pores of most known MOFs is a serious limitation. The recently developed method denoted as the *de novo* approach could solve this problem. In this method, the crystals of MOFs grow around the enzyme molecules under mild reaction conditions. For this purpose, in the resumption of our previously published papers on the preparation of the lipase@ZIF-67 biocatalyst[21] and bovine carbonic anhydrase (BCA)@ZIF-8,[22] the *de novo* approach was selected, which allows for the suitable protection of the enzyme to avoid leaching. Therefore, we herein report the green one-pot bottle-around-ship synthesis of a heterogeneous biocatalyst based on the CRL within the ZIF-8. In this method, precursors of ZIF-8 (bottle) and CRL (ship) are placed in the reaction vessel. The MOF structure is constructed around the enzyme species. It is clear that in this method, the procedure for MOF synthesis should be chosen, so that the encapsulated enzymes are not destroyed and their activity is not reduced. The superior properties of the synthesized biocatalyst have been investigated in the synthesis of lactose caprate by enzymatic esterification of lactose with capric acid. The resulting product was analyzed using HPLC, and then the synthesized lactose caprate ester was utilized as an anticancer agent. There is a limited number of studies dealing with the potential applications of lactose-based surfactants for pharmaceutical applications.[7,10] According to the World Health Organization statistics, cancer has been known as one of the major causes of death in the world. The traditional therapeutic ways to eliminate cancer cells generate high toxicity. Therefore, the development of new drugs with less toxicity and greater efficacy is highly necessary for clinical treatment. To take a step on this purpose, the activity of the lactose caprate against two human cancer cell lines, HeLa carcinoma and K562 leukemia, was tested.

2 Experimental

2.1. Materials

Lipase from *Candida rugosa* (lyophilized powder, type VII, nominal activity $\gg$ 700 U mg^{-1}), *para*-nitro phenol, bovine serum albumin (BSA), Coomassie brilliant blue G-250, RPMI 1640 medium, 2-methylimidazole (Hmim, 98%), Triton X-100, and 3-(4,5-dimethylthiazol-2-yl)-2,5-diphenyltetrazolium bromide (MTT) were purchased from Sigma-Aldrich Chemical Company. $Zn(NO_3)_2 \cdot 6H_2O$ ($\geq$99.5%) was supplied by Sinopharm Chemical Reagent Co., Ltd. *Para*-nitro phenyl palmitate (*p*-NPP), molecular sieve, capric acid, and lactose caprate were purchased from Merck company. Fetal calf serum (FCS) was provided by Gibco (Germany) and Arabic gum was provided by Carlo Erba.

2.2. Characterization

Powder X-ray diffraction (XRD) patterns of the samples were recorded using a Bruker D8 Advance instrument with Cu K_α (λ = 1.5406 Å) radiation. Specific surface area, pore volume and pore size were measured by adsorption–desorption of N_2 gas at 77.360 K using an ASAP 2000 Micromeritics instrument. Diffuse reflectance Fourier transform infrared (DR-FTIR) spectroscopy was performed using a JASCO FT/IR 6300 spectrometer in the range of 4000–400 cm^{-1}. A Hitachi S-4700 field emission-scanning electron microscope (FE-SEM) and a JASCO V-570 spectrophotometer were used for acquiring the scanning electron micrographs and the UV-Vis spectra, respectively. The absorbance optical density was read at 570 nm using an ELISA reader from BioTek, Winooski, VT.

2.3. Biocatalyst preparation

2.3.1. ZIF-8. A modified procedure was followed for the preparation of ZIF-8.[23] In short, $Zn(NO_3)_2 \cdot 6H_2O$ (0.059 g, 0.198 mmol) was dissolved in 4 mL deionized water and added to 8 mL aqueous solution of 2-methylimidazole (1.135 g, 13.82 mmol) under stirring. The reaction mixture was left under continuous stirring for 24 hours. The as-synthesized ZIF-8 solid was separated by centrifugation (5000 rpm, 10 min) and washed three times with deionized water.

2.3.2. CRL@ZIF-8. In a typical experiment, aqueous solutions of CRL (10 mg), $Zn(NO_3)_2 \cdot 6H_2O$ (0.059 g), and 2-methylimidazole (1.135 g) were added to a round-bottom flask and kept at 25 °C for 24 h under stirring. The obtained CRL@ZIF-8 composite was separated by centrifugation at 5000 rpm for 10 min and then washed three times with deionized water.

The Bradford method was applied for the determination of protein content.[24] The efficiency of the encapsulated enzyme was calculated using the following formula:[25]

$$\text{Enzyme encapsulation efficiency}\% = (C_1V_1 - C_2V_2) \div (C_1V_1) \times 100 \quad (1)$$

C_1 (mg mL^{-1}) and C_2 (mg mL^{-1}) refer to the primary and final concentrations of the enzyme, respectively. V_1 (mL) and V_2 (mL) are the volumes of the enzyme solution used for encapsulation and the supernatant after encapsulation, respectively.

2.4. Lipase activity assay

The activity of free and encapsulated CRL was assayed spectrophotometrically by the hydrolysis of *p*-NPP, which shows a rise in the absorption band at 405 nm. The activity of free and encapsulated CRL was measured by adding 2 mg free CRL or 20 mg CRL@ZIF-8 to the assay mixture, consisting of the following two solutions: solution I (30 mg *p*-NPP in 10 mL isopropanol) and solution II (0.1 g Arabic gum and 0.4 mL Triton X-100 in 90 mL phosphate buffer; 50 mM, pH 7). The assay mixture was incubated at 37 °C under 400 rpm for 5 min, and both free and encapsulated CRL catalyzes the formation of *p*-nitrophenol, which was quantified at $\lambda = 405$ nm at room temperature. The amount of CRL which forms 1 μmol of *p*-nitrophenol per minute under assay conditions is considered as the one unit of CRL activity (1 U).

2.5. Kinetic parameters

The Michaelis–Menten kinetics was applied to describe the dependence of enzymatic activity on the substrate concentration. The enzymatic activity was determined based on "Lipase activity assay" section. The kinetic parameters (K_m and V_{max}) of free and immobilized CRL were determined using the Lineweaver–Burk equation as follows:

$$1/V = (1/V_{max}) + (K_m/V_{max}[S]) \quad (2)$$

where V is the initial reaction rate for different concentrations of substrates; $[S]$ is the initial concentration of the substrate; V_{max} (mM min^{-1}) and K_m (mM) are the maximum reaction rate and Michaelis–Menten constant respectively.

2.6. Effect of pH

The effect of the pH on the CRL stability and the protection provided by the MOF were determined by incubating the free (2 mg) and encapsulated CRL (20 mg CRL@ZIF-8) in 2 mL of 50 mM PBS solution in the range of pH 2.0 to 9.0 adjusted by adding HCl (0.1 M) and NaOH (0.1 M) solutions at room temperature (RT). Then, the relative activates were evaluated as previously described in Section 2.4.

2.7. Thermal stability

To investigate the thermal stability of the free and encapsulated CRL, its free (2 mg) and encapsulated forms (20 mg CRL@ZIF-8) were incubated in 50 mM PBS at pH = 7 in the temperature range of 30 to 60 °C for 1 h. Then, the relative activities were measured as mentioned above.

2.8. Synthesis of sugar fatty acid esters

The enzymatic esterification reaction was carried out in a round-bottom flask containing of lactose and capric acid (different molar ratios in the range of 3/1 to 1/3), molecular sieve (1.5 g) and CRL@ZIF-8 (varying amount from 10 to 30 mg) in acetone (10.0 mL) at mild temperatures (40–60 °C) for different times (12–60 h) in order to optimize the reaction conditions. After the reaction, the mixture was centrifuged at 8000 rpm for 5 min. In the subsequent stage, the acetone layer was evaporated and the mobile phase methanol : acetonitrile : water (40 : 35 : 25) was added to the reaction media. The reaction conversion was measured based on the remaining free fatty acid in the reaction media using HPLC. The pure ester product was extracted by *n*-hexane and examined as an anticancer agent.

2.9. HPLC determination of lactose ester

HPLC analysis of lactose ester was performed using a PerfectSil Target ODS-C18 (150 × 4.6 mm) (particle size 5 μm) column maintained at 40 °C using a UV-Vis detector. The mobile phase was methanol : acetonitrile : water (40 : 35 : 25) at a flow rate of 1 mL min^{-1}.

The conversion efficiency was calculated based on the reduction in capric acid concentration as determined by HPLC using calibration standards of the acid as reference:

$$C = (A_{ca0} - A_{cat})/A_{ca0} \quad (3)$$

where C is the conversion ratio, A_{ca0} is the peak area of the free capric acid at $t = 0$; A_{cat} is the peak area of capric acid at the specified reaction time.

2.10. Reusability of the biocatalyst

The reusability of the CRL@ZIF-8 catalyst was evaluated in the esterification reaction of lactose with capric acid under the optimum conditions. When the reaction was done, the biocatalyst was recovered by centrifugation (8000 rpm, 5 min), washed with acetone, and dried at RT before the next reaction cycle. The structure and porosity of the recovered biocatalyst was monitored by XRD, FT-IR spectroscopy, and N_2 adsorption–desorption analysis after the last cycle.

2.11. Cell culture and MTT assay

Two human cancer cell lines including K562 myelogenous leukemia and HeLa cervix carcinoma were used to evaluate the growth inhibitory effect of lactose caprate. Cells were cultured in an RPMI-1640 medium supplemented with 10% FCS and antibiotics in a culture flask, and incubated at 37 °C in a humidified CO_2 incubator. When the cells were confluent and the viability was ≥95%, they were used for the MTT cytotoxicity assay. K562 and HeLa cells at concentrations of 7000 cells per well were cultured in 96-well plates in triplicate and treated with 1–200 μg mL^{-1} of the compound at 37 °C for 48 h with 5% CO_2. Cells untreated with the compound were considered as the negative control. Then, 10 μL MTT (5 mg mL^{-1}) was added to each well and the cells were incubated at 37 °C for 4 h. The supernatant of the cells was removed and 150 μL dimethyl sulphoxide (DMSO) was added and shaken for 15 min to dissolve the generated crystals. The absorbance of each well was read at 570 nm with a reference wavelength of 690 nm using an

ELISA reader. The cell growth inhibition percentage was calculated using the following formula:

$$100 - [(\text{absorbance of test sample/absorbance of negative control sample}) \times 100] \quad (4)$$

Statistical analysis was performed using the SPSS software and the one-way ANOVA. *P* values less than 0.5 were considered as significant.

The fifty percent inhibitory concentration (IC_{50}) of the compound was determined using the Curve Expert software.

3 Results and discussion

3.1. Synthesis and characterization of CRL@ZIF-8

In this work, owing to the inaccessibility of the six-ring windows of ZIF-8 pores for the selected large size enzyme (5.2 nm), the "bottle-around-ship" strategy in a green system with an aqueous solution and room temperature conditions was employed for the encapsulation of CRL into ZIF-8. A CRL loading of 15.56 wt% in CRL@ZIF-8 was calculated using a standard Bradford assay method. The activity of the encapsulated enzyme was measured to be 72.4% compared to the equivalent free enzyme by the hydrolysis of *p*-NPP to *p*-nitrophenol. The resulting biocatalyst was entirely characterized by various techniques including XRD, FT-IR, FE-SEM, and N_2 adsorption–desorption.

As shown in Fig. 1, the XRD pattern of CRL@ZIF-8 is in good agreement with that of ZIF-8, which indicates that CRL enzyme encapsulation inside ZIF-8 pores has no impact on its crystal.

The FT-IR spectra of the ZIF-8, CRL and composite biocatalyst are shown in Fig. 2. The strong absorption bands at 758 and 692.4 cm^{-1} are ascribed to the out-of-plane bending of the imidazole aromatic ring, whereas the bands at 1350–1500 cm^{-1} belong to the in-plane bending of the ring (Fig. 2c). The band at 1574 cm^{-1} is associated with the stretching mode of C=N in 2-MIM and the stretching mode of imidazole ring shows a band at 1420 cm^{-1}. Finally, the characteristic band at 421 cm^{-1} can be assigned to the Zn–N stretching mode.[26] As shown in Fig. 2b, the CRL@ZIF-8 spectrum exhibits one absorption peak at 1657 cm^{-1} corresponding to the C=O stretching vibration mode in amide I bonds, which confirms the successful encapsulation of CRL molecules in ZIF-8. There is a slight shift of the amide I peak in CRL@ZIF-8, which confirmed a direct enzyme-MOF interaction due to the coordination between Zn^{2+} and the carbonyl groups on the enzyme.[27] This covalent bonding, along with hydrogen bonding and hydrophobic interactions previously reported, inevitably caused an alteration in the conformational integrity of enzyme molecules.[28]

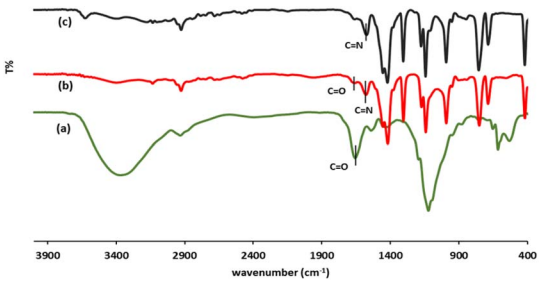

Fig. 2 FT-IR spectra of free CRL (a), CRL@ZIF-8 composite (b) and ZIF-8 (c).

The N_2 adsorption–desorption isotherms of ZIF-8 display a typical type I isotherm associated with a microporous material (Fig. 3) with a high surface area of 1340 $m^2\ g^{-1}$ and a total pore volume of 0.638 $cm^3\ g^{-1}$. Compared to ZIF-8, a surface area of 572 $m^2\ g^{-1}$ and a total pore volume of 0.47 $cm^3\ g^{-1}$ was obtained for CRL@ZIF-8, which indicate a noticeable decrease owing to enzyme encapsulation into the ZIF-8 pores.

The SEM images of pure ZIF-8 and washed CRL@ZIF-8 biocatalysts are shown in Fig. 4, which indicate negligible changes in the morphology of ZIF-8 after enzyme encapsulation. The successful encapsulation of CRL into the MOF structure without affecting ZIF-8 stability and crystallinity was confirmed by comparing the SEM images and XRD patterns of ZIF-8 with enzyme-containing ZIF-8 samples. However, we cannot exclude the presence of structural defects and/or a small amount of amorphous hybrid solids.[29] In a *de novo* approach, the existence of a somewhat amorphous structure in the hybrid solid cannot be ignored because of the presence of the CRL enzyme in the crystal growth process of ZIF-8. However, the rhombic dodecahedral shape and smooth

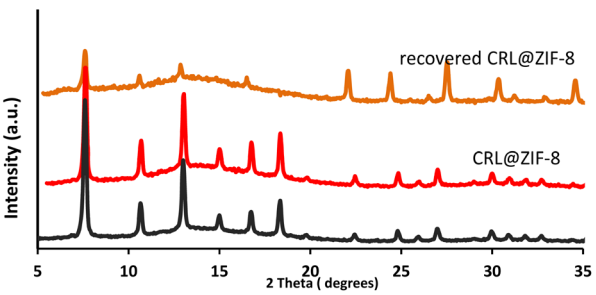

Fig. 1 PXRD patterns of ZIF-8, CRL@ZIF-8 and recovered CRL@ZIF-8.

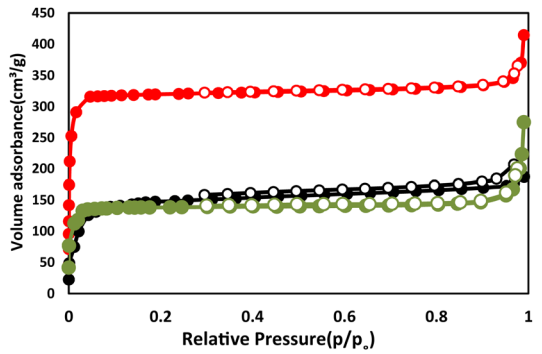

Fig. 3 N_2 adsorption–desorption isotherms for ZIF-8 (red), CRL@ZIF-8 (green) and recovered CRL@ZIF-8 (black) at 77 K. The filled and empty circles represent adsorption and desorption branches, respectively.

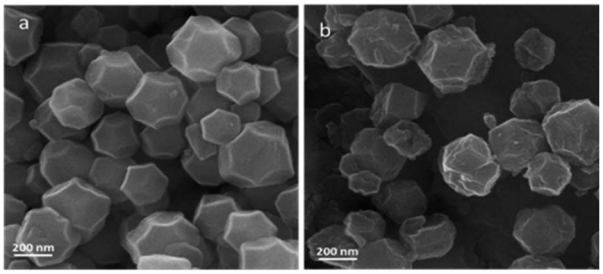

Fig. 4 FE-SEM images of (a) pure ZIF-8 and (b) CRL@ZIF-8.

surface of pure ZIF-8 crystals would be blurred to some extent by enzyme encapsulation into ZIF-8.[27]

3.2. Effect of pH and temperature on the activity of encapsulated CRL

One of the key parameters for the successful application of the enzyme is stability. It is expected that enzyme encapsulation improves its stability and activity in a wide range of pH and temperature, and in various organic solvents compared to the free enzyme. To confirm the protective effect of the framework on the enzyme, the final activity of CRL@ZIF-8 was evaluated after its exposure to different pH values in the range of 2 to 9. The obtained results in Fig. 5b indicate that there is no significant changes in the relative activity (the maximum observed activity has been defined as 100% for comparison purposes) of free CRL toward encapsulated CRL within the pH range of 6–7. However, the higher activity for CRL@ZIF-8 than that of the free CRL in acidic (2–6) and alkali (7–9) regions approved the positive effect of enzyme encapsulation in its performance.

The effect of temperature on the activity of free and encapsulated CRL in the temperature range of 30–60 °C is shown in Fig. 5a. The relative activity of the free and encapsulated CRL is the same up to 35 °C. By further increasing the temperature from 35 to 65 °C, the activity of both free and stabilized enzymes decreases, but the rate of decrease for the free CRL is higher than that of the encapsulated one. For instance, the free CRL retained only 31% of its initial activity, whereas for the encapsulated CRL, this value was 62% at 55 °C. Therefore, the encapsulation of the enzyme seems to prevent its conformation transition at high temperatures and enhance its thermal stability. The activity loss of the enzyme at high temperatures is associated with its conformational transitions, which is considerably decreased by the immobilization strategy.

3.3. Reusability of immobilized CRL

In order to investigate the reusability of immobilized CRL, the synthesized CRL@ZIF-8 was separated from *p*-NPP hydrolysis reaction media and, after washing with phosphate buffer, reused in the next run with a fresh substrate. The recovery and reuse processes were repeated until 6 cycles and the obtained results are displayed in Fig. 5c. The biocatalyst activity decreased to 63% of the initial activity after 6 cycles. However, the relative activity of CRL@ZIF-8 does not indicate a significant decrease.

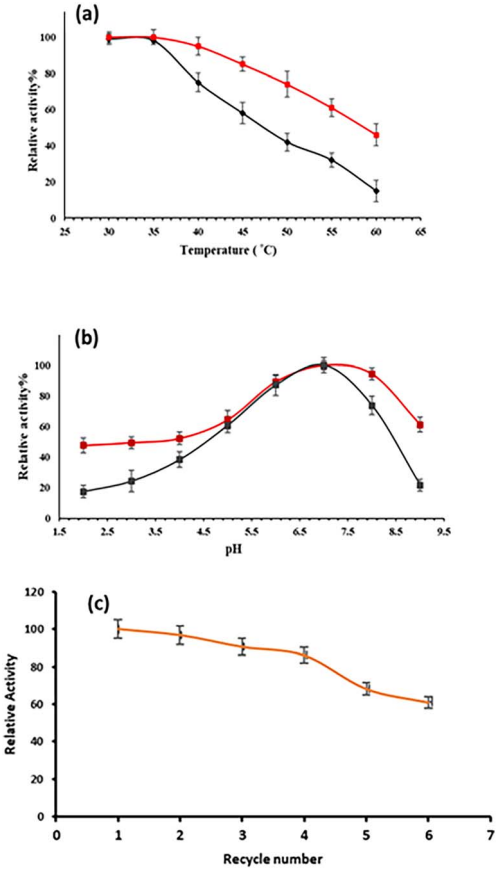

Fig. 5 The effect of temperature (a) and pH (b) on the enzymatic activity of free CRL (black) and CRL@ZIF-8 (red) and reusability of the immobilized CRL (c).

3.4. Kinetics studies

The Michaelis–Menten kinetic parameters of free CRL and immobilized CRL (CRL@ZIF-8) were calculated, and the results are summarized in Table 1. The K_m value is the substrate concentration at which the reaction rate is half of V_{max} and shows the affinity of the enzyme for the substrate. The K_m values are 0.0602 and 0.7285 mM, for free CRL and CRL@ZIF-8, respectively. This increase in K_m value might be either due to the structural changes in the enzyme induced by the applied immobilization procedure or due to the lower accessibility of the substrate to the active sites of the immobilized enzyme.[30] A similar result involving an increase in the K_m value of CRL after immobilization has been reported in the literature.[31] V_{max} stands for the highest rate of enzymatic reaction when the enzyme is saturated with the substrate. The V_{max} value was improved from 3.796×10^{-3} for free CRL to 4.343×10^{-3} for CRL@ZIF-8.

Table 1 Kinetic parameters of free CRL and CRL@ZIF-8

	K_m (mM)	V_{max} (mM min^{-1})
Free CRL	0.0602	3.796×10^{-3}
CRL@ZIF-8	0.7285	4.343×10^{-3}

3.5. Synthesis of sugar fatty acid esters

In contrast to the chemical synthesis, the enzyme-catalyzed processes are remarkably more selective for the synthesis of sugar esters. The lipase-catalyzed regioselective esterification of the lactose sugar seems to be a better alternative to chemical synthesis as it requires a lower reaction temperature and a high operational enzyme stability comparatively, thereby producing a higher yield of sugar esters.[10,32] The obtained ester was characterized by FTIR spectroscopy. The characteristic absorbance bands in the FTIR spectra in Fig. S1† confirm the formation of lactose caprate. The hydroxyl group (–OH) absorption of lactose at 3300–3400 cm^{-1} is observed in lactose caprate ester (Fig. S1c†). The sharp band at 2930 cm^{-1} is due to the two types of C–H bonds located in the glucose and galactose units and the functional groups outside the sugars.[33] The carbonyl bond of capric acid at 1710 cm^{-1} exists in the lactose caprate spectra, which strongly suggest the existence of the corresponding ester due to the new bond (COO–R) formed by the esterification process. Fig. S2† shows the HPLC chromatograms of the reaction mixture for the synthesis of lactose caprate using CRL@ZIF-8 in acetone. The peak area of the remaining capric acids was used to determine the conversion rate of capric acid using a calibration curve. The peaks at a retention time of 1–3.5 minutes correspond to lactose and solvents and the peaks at retention time around 4 minute corresponds to lactose caprate. The analysis showed monocaprate ester to be the main product (92%), which appeared at the retention time very close to that of the free sugar. As shown, the reaction catalyzed by this immobilized CRL was very selective towards the formation of monoester.

Here we studied the effect of different reaction parameters including the amount of biocatalysts, substrate molar ratio, temperature, and time to optimize the esterification reaction using the CRL@ZIF-8 composite for the production of lactose ester. It should be noted that capric acid and lactose with a small dimension, about 0.86 Å,[34] can easily diffuse into the pores of the CRL@ZIF-8 composite.

3.5.1. Effect of substrate molar ratios. The relative proportions of various substrates are a key parameter in the enzymatic sugar ester synthesis, since the molar ratio of the reacting substrates significantly influences the physical and chemical properties of the reaction mixture. In this regard, the effect of lactose-to-capric acid molar ratios was examined in the range of 3 : 1 to 1 : 3. The highest conversion efficiency was achieved at 2 : 1 molar ratio of lactose (3.2 mg, 9.3 μmol) to capric acid (0.8 mg, 4.6 μmol), with almost 92% conversion. A further increase in lactose concentration dramatically decreased the conversion rate, as shown Fig. 6a. The presence of an excessive amount of sugar can promote the transformation of fatty acid, potentially resulting in the generation of by-products instead of the desired sugar ester. Nonetheless, the inclusion of solid sugar in the reaction medium may impact the enzyme's effectiveness.[18] When the ratio of sugar to capric acid is within the range of 1 : 1 to 1 : 2, the conversions were decreased, as a result of acid inhibition, and then an increase was observed in 1 : 3. In previous studies, it has been observed that the catalytic activity of immobilized lipase in the esterification of sugars and fatty acids is enhanced

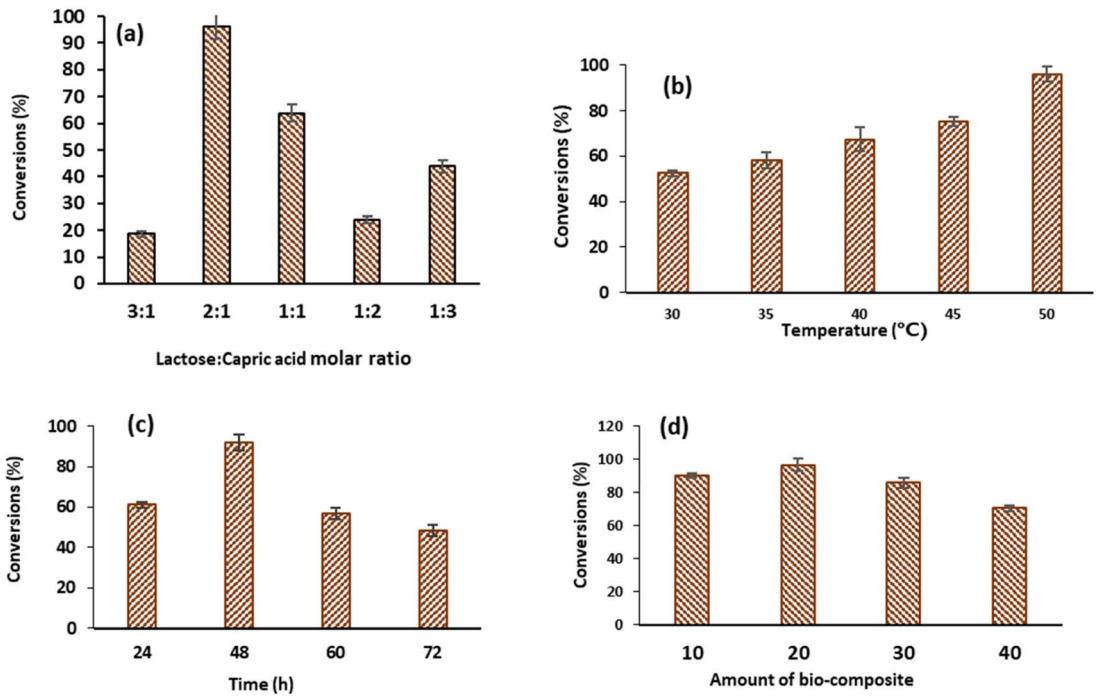

Fig. 6 The effect of lactose-to-capric acid molar ratio (a), temperature (b), time (c) and biocatalyst amount (d) on the enzymatic synthesis of sugar esters. The enzymatic esterification reaction involves lactose (3.2 mg, 9.3 μmol), capric acid (0.8 mg, 4.6 μmol), a molecular sieve (1.5 g), and a biocatalyst (20 mg) in acetone (50.0 mL) at 50 °C for 48 h at a shaking speed of 400 rpm.

when the concentration of the acyl donor is higher than that of the sugar.[35] The equilibrium constant of the esterification reaction is affected by the concentrations of the reactants. When lipases are immobilized, they can change their shape and behavior due to interactions with lipophilic substances. This includes a movement in a loop structure called an α-helical loop.[36]

3.5.2. Effects of temperature. Another crucial parameter that can affect the stability of the enzyme, as well as the rate of the reaction and position of the equilibrium, is the reaction temperature. In this regard, the enzymatic esterification was evaluated at different reaction temperatures to determine the optimum reaction temperature. For the enzymatic synthesis of lactose esters, Zaidan *et al.*[18] reported a decrease in the CRL activity upon increasing the temperature from 45 to 60 °C, which was related to CRL denaturation at higher temperatures while our synthesized biocatalyst demonstrated the highest ester conversion at 50 °C, which was selected as the optimized, with almost 92% conversion efficiency (Fig. 6b). Therefore, the use of CRL in encapsulated forms into the MOF matrix shows more thermal stability and provides more potential for commercial biotechnological applications than the free CRL.

3.5.3. Effect of time. The effect of the reaction time as an important factor on the enzymatic synthesis of lactose ester was investigated (Fig. 6c). The conversion efficiency increased by increasing the time period from 24 to 48 h. Extending the reaction time to more than 48 h caused a considerable decrease in the conversion efficiency, which dropped down to 48%.

3.5.4. Effect of biocatalyst amounts. Fig. 6d shows the effect of the amount of CRL@ZIF-8 on the reaction conversion. It is clear that with the increase in the amount of biocatalyst to 20 mg, the conversion also increased but a further increase in the amount of biocatalyst to 30 and 40 mg decreased the conversion efficiency, which can be due to mass transfer limitation in the pores.

3.6. Biocatalyst recovery and reuse

Generally, immobilized enzymes are considered proper biocatalysts from an industrial point of view, when they can be easily recovered from the reaction mixtures and reused. For this reason, the recyclability of the prepared biocatalyst was evaluated in sequential esterification reactions. Hence, CRL@ZIF-8 was separated from the reaction media by simple centrifugation, washed carefully with acetone and reused for a new reaction cycle. Interestingly, it was found that the prepared biocatalyst retained 68% of its activity after 6 cycles. This remarkable recyclability could be assigned to the protection of enzyme from direct inactivation, which is related to the encapsulation of CRL within the ZIF-8 matrix. The amount of CRL in the filtrate after the recycling test was determined by the Bradford method, which confirmed the absence of any enzyme leaching in the solution. The decrease in the enzymatic activity could be due to the denaturation of enzymes after several cycles.[37] For more investigation on the structural stability of the recovered biocatalyst, the XRD pattern was recorded after the final run (Fig. 1), which indicated that the structure was preserved after reuse.

3.7. Effect of lactose caprate on cell proliferation

Growing concerns about global cancer rates as one of the major public health problems have led to challenges worldwide, necessitating the design and synthesis of novel molecules as anticancer agents. Carbohydrate esters are considered potential anticancer agents due to their low toxicity, non-antigenicity and biodegradability. Additionally, it is clear from the work of various authors that cancer cells overexpress sugar transporters, which is why sugar fatty acid esters represent themselves as good candidates to act as anticancer agents.[38] As part of our investigation on a novel application of sugar esters, the activity of the lactose caprate against two human cancer cell lines, HeLa carcinoma and K562 leukemia, was tested. As shown in Fig. 7, this compound has inhibitory effects on the growth of both K562 and HeLa cancer cells. This effect was concentration dependent, so that the highest inhibition was observed at a concentration of 200 μg mL^{-1}. The calculation of IC_{50} values after 48 h of cell exposure to the compound showed IC_{50} values of 49.6 ± 1.3 μg mL^{-1} (0.1 ± 0.002 μM) for K562 cells and 57.2 ± 1.8 μg mL^{-1} (0.115 ± 0.003 μM) for HeLa cells, which indicated the antitumor effects of the lactose caprate against both cell lines.

To compare the cytotoxic effect of lactose caprate with the reported antitumors for HeLa and K562 cell lines, the measured IC_{50} values for the compounds are summarized in Table 2. These results displayed that the IC_{50} value for lactose caprate is lower than that of the previously reported drugs, indicating that lactose caprate is a potential anticancer.

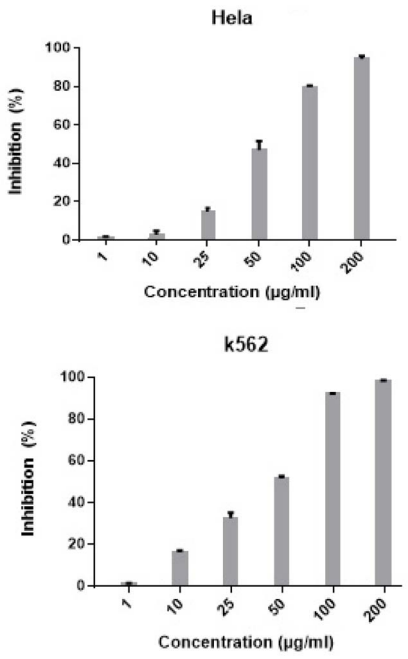

Fig. 7 Inhibitory effect of lactose caprate on K562 and HeLa cancer cells after 48 hours of treatment. The values represent the mean of different experiments. Lactose caprate at concentrations more than 10 μg mL^{-1} significantly inhibited the proliferation of treated HeLa and K562 cells compared to untreated cells ($p < 0.05$).

Table 2 IC_{50} (μM) values for various compounds against HeLa and K562 cell lines

Antitumor (MTT assay, 48 h)	HeLa	K562	Reference
Lactose caprate	0.115 ± 0.003	0.1 ± 0.002	This work
Doxorubicin	3.56 ± 2.7	—	39
5-Fluorouracil	2.78 ± 2.6	—	39
Cytarabine	464.433 ± 10.009	—	40
Cisplatin	8.41 ± 0.18	10.78 ± 0.94	41
$[Cu(theophylline)_2(H_2O)_3]$	—	11.7	42

4 Conclusions

In conclusion, the CRL enzyme has been encapsulated into ZIF-8 frameworks *via* the "bottle-around-ship" strategy. The obtained CRL@ZIF-8 composite was applied as a heterogeneous catalyst for lactose caprate synthesis *via* the esterification of lactose with capric acid. The ZIF-8 framework provided high thermal and chemical stability and reusability for the CRL enzyme. The most obvious finding of this study was the inhibitory effect of the produced lactose caprate on K562 leukemia and HeLa cancer cells. The synthesized lactose caprate demonstrated an extraordinary cytotoxicity profile and anticancer effects against both K562 leukemia and HeLa cancer cell lines. Taken together, these findings suggest a role for lactose caprate in promoting pharmaceutical ingredients.

Author contributions

S. T., M. M., and V. M. conceived this project. E. K. and S. R. performed the materials synthesis and characterization. I. M. designed the sugar fatty acid ester synthesis reaction conditions and Z. A. conducted the anticancer tests. The data were analyzed by all authors. A. M. and R. K. wrote and edited the manuscript. All authors discussed the results and commented on the manuscript.

Conflicts of interest

There are no conflicts to declare.

Acknowledgements

We are grateful to the Research Council of the University of Isfahan for financial support of this work.

Notes and references

1 M. Ferrer, J. Soliveri, F. J. Plou, N. López-Cortés, D. Reyes-Duarte, M. Christensen, J. L. Copa-Patiño and A. Ballesteros, Synthesis of sugar esters in solvent mixtures by lipases from Thermomyces lanuginosus and Candida antarctica B, and their antimicrobial properties, *Enzyme Microb. Technol.*, 2005, **36**, 391–398.

2 J. F. Kennedy, H. Kumar, P. S. Panesar, S. S. Marwaha, R. Goyal, A. Parmar and S. Kaur, Enzyme-catalyzed regioselective synthesis of sugar esters and related compounds, *J. Chem. Technol. Biotechnol.*, 2006, **81**, 866–876.

3 S. J. Marathe, N. Dedhia and R. S. Singhal, Esterification of sugars and polyphenols with fatty acids: techniques, bioactivities, and applications, *Curr. Opin. Food Sci.*, 2022, **43**, 163–173.

4 S. J. Marathe, N. N. Shah and R. S. Singhal, Enzymatic synthesis of fatty acid esters of trehalose: process optimization, characterization of the esters and evaluation of their bioactivities, *Bioorg. Chem.*, 2020, **94**, 103460.

5 U. T. Bornscheuer, G. R. Ordoñez, A. Hidalgo, A. Gollin, J. Lyon, T. S. Hitchman and D. P. Weiner, Selectivity of lipases and esterases towards phenol esters, *J. Mol. Catal. B: Enzym.*, 2005, **36**, 8–13.

6 S. Šabeder, M. Habulin and Ž. Knez, Comparison of the esterification of fructose and palmitic acid in organic solvent and in supercritical carbon dioxide, *Ind. Eng. Chem. Res.*, 2005, **44**, 9631–9635.

7 M. Verboni, S. Lucarini and A. Duranti, 6′-O-Lactose ester surfactants as an innovative opportunity in the pharmaceutical field: from synthetic methods to biological applications, *Pharmaceuticals*, 2021, **14**, 1306.

8 M. Enayati, Y. Gong, J. M. Goddard and A. Abbaspourrad, Synthesis and characterization of lactose fatty acid ester biosurfactants using free and immobilized lipases in organic solvents, *Food Chem.*, 2018, **266**, 508–513.

9 F. Scholnick, M. Sucharski and W. Linfield, Lactose-derived surfactants (I) fatty esters of lactose, *J. Am. Oil Chem. Soc.*, 1974, **51**, 8–11.

10 J. Staroń, J. M. Dąbrowski, E. Cichoń and M. Guzik, Lactose esters: synthesis and biotechnological applications, *Crit. Rev. Biotechnol.*, 2018, **38**, 245–258.

11 S. Lucarini, L. Fagioli, R. Cavanagh, W. Liang, D. R. Perinelli, M. Campana, S. Stolnik, J. K. Lam, L. Casettari and A. Duranti, Synthesis, structure–activity relationships and *in vitro* toxicity profile of lactose-based fatty acid monoesters as possible drug permeability enhancers, *Pharmaceutics*, 2018, **10**, 81.

12 S. Maher, R. J. Mrsny and D. J. Brayden, Intestinal permeation enhancers for oral peptide delivery, *Adv. Drug Delivery Rev.*, 2016, **106**, 277–319.

13 D. R. Perinelli, D. Vllasaliu, G. Bonacucina, B. Come, S. Pucciarelli, M. Ricciutelli, M. Cespi, R. Itri, F. Spinozzi and G. F. Palmieri, Rhamnolipids as epithelial permeability enhancers for macromolecular therapeutics, *Eur. J. Pharm. Biopharm.*, 2017, **119**, 419–425.

14 B. Pérez, S. Anankanbil and Z. Guo, Synthesis of sugar fatty acid esters and their industrial utilizations, *Fatty Acids*, 2017, pp. 329–354.
15 R. Sharma, Y. Chisti and U. Banerjee, Production, purification, properties of induced lipases, *Biotechnol. Adv.*, 2001, **19**, 627–662.
16 E. Vanleeuw, S. Winderickx, K. Thevissen, B. Lagrain, M. Dusselier, B. P. Cammue and B. F. Sels, Substrate-specificity of *Candida rugosa* lipase and its industrial application, *ACS Sustain. Chem. Eng.*, 2019, **7**, 15828–15844.
17 J.-Y. Yue, X.-L. Ding, L. Wang, R. Yang, J.-S. Bi, Y.-W. Song, P. Yang, Y. Ma and B. Tang, Novel enzyme-functionalized covalent organic frameworks for the colorimetric sensing of glucose in body fluids and drinks, *Mater. Chem. Front.*, 2021, **5**, 3859–3866.
18 U. H. Zaidan, M. B. A. Rahman, S. S. Othman, M. Basri, E. Abdulmalek, R. N. Z. R. A. Rahman and A. B. Salleh, Biocatalytic production of lactose ester catalysed by mica-based immobilised lipase, *Food Chem.*, 2012, **131**, 199–205.
19 S. Dutta and I. S. Lee, Metal–organic framework based catalytic nanoreactors: synthetic challenges and applications, *Mater. Chem. Front.*, 2021, **5**, 3986–4021.
20 S. S. Nadar, L. Vaidya and V. K. Rathod, Enzyme embedded metal organic framework (enzyme–MOF): *de novo* approaches for immobilization, *Int. J. Biol. Macromol.*, 2020, **149**, 861–876.
21 S. Rafiei, S. Tangestaninejad, P. Horcajada, M. Moghadam, V. Mirkhani, I. Mohammadpoor-Baltork, R. Kardanpour and F. Zadehahmadi, Efficient biodiesel production using a lipase@ZIF-67 nanobioreactor, *Chem. Eng. J.*, 2018, **334**, 1233–1241.
22 V. Asadi, R. Kardanpour, S. Tangestaninejad, M. Moghadam, V. Mirkhani and I. Mohammadpoor-Baltork, Novel bovine carbonic anhydrase encapsulated in a metal–organic framework: a new platform for biomimetic sequestration of CO_2, *RSC Adv.*, 2019, **9**, 28460–28469.
23 Y. Pan, Y. Liu, G. Zeng, L. Zhao and Z. Lai, Rapid synthesis of zeolitic imidazolate framework-8 (ZIF-8) nanocrystals in an aqueous system, *Chem. Commun.*, 2011, **47**, 2071–2073.
24 M. M. Bradford, A rapid and sensitive method for the quantitation of microgram quantities of protein utilizing the principle of protein-dye binding, *Anal. Biochem.*, 1976, **72**, 248–254.
25 M. Aghababaie, M. Beheshti, A. Razmjou and A.-K. Bordbar, Covalent immobilization of *Candida rugosa* lipase on a novel functionalized Fe_3O_4@SiO_2 dip-coated nanocomposite membrane, *Food Bioprod. Process.*, 2016, **100**, 351–360.
26 L. B. Vaidya, S. S. Nadar and V. K. Rathod, Entrapment of surfactant modified lipase within zeolitic imidazolate framework (ZIF)-8, *Int. J. Biol. Macromol.*, 2020, **146**, 678–686.
27 L. Qi, Z. Luo and X. Lu, Biomimetic mineralization inducing lipase–metal–organic framework nanocomposite for pickering interfacial biocatalytic system, *ACS Sustain. Chem. Eng.*, 2019, **7**, 7127–7139.
28 S. S. Nadar, S. D. Gawas and V. K. Rathod, Self-assembled organic inorganic hybrid glucoamylase nanoflowers with enhanced activity and stability, *Int. J. Biol. Macromol.*, 2016, **92**, 660–669.
29 X. Wu, C. Yang and J. Ge, Green synthesis of enzyme/metal-organic framework composites with high stability in protein denaturing solvents, *Bioresour. Bioprocess.*, 2017, **4**, 1–8.
30 S.-H. Chiou and W.-T. Wu, Immobilization of *Candida rugosa* lipase on chitosan with activation of the hydroxyl groups, *Biomaterials*, 2004, **25**, 197–204.
31 E. Ozyilmaz, O. Caglar, I. Sargin and G. Arslan, Synergistic role of carbon quantum dots in the activity and stability of *Candida rugosa* lipase encapsulated within metal–organic frameworks (ZIF-8), *Mater. Today Commun.*, 2022, **30**, 103066.
32 J. L. Gonzalez-Alfonso, L. Casas-Godoy, J. Arrizon, D. Arrieta-Baez, A. O. Ballesteros, G. Sandoval and F. J. Plou, in *Lipases and Phospholipases*, Springer, 2018, pp. 287–296.
33 W. B. Nicely, in *Advances in carbohydrate chemistry*, Elsevier, 1957, vol. 12, pp. 13–33.
34 K. Saraboji, M. Håkansson, S. Genheden, C. Diehl, J. Qvist, U. Weininger, U. J. Nilsson, H. Leffler, U. Ryde and M. Akke, The carbohydrate-binding site in galectin-3 is preorganized to recognize a sugarlike framework of oxygens: ultra-high-resolution structures and water dynamics, *Biochemistry*, 2012, **51**, 296–306.
35 R. Gulati, P. Arya, B. Malhotra, A. K. Prasad, R. K. Saxena, J. Kumar, A. C. Watterson and V. S. Parmar, Novel biocatalytic esterification reactions on fatty acids: synthesis of sorbitol 1 (6)-monostearate, *Arkivoc*, 2003, **3**, 159–170.
36 J.-P. Chen and W.-S. Lin, Sol-gel powders and supported sol-gel polymers for immobilization of lipase in ester synthesis, *Enzyme Microb. Technol.*, 2003, **32**, 801–811.
37 Y. Xiao, Y. Chen, R. Lu, Y. Wang and C. Wang, Immobilization of *Candida rugosa* lipase (CRL) on a hierarchical magnetic zeolitic imidazole framework-8 for efficient biocatalysis, *Biochem. Eng. J.*, 2021, **175**, 108120.
38 C. F. Higgins, Multiple molecular mechanisms for multidrug resistance transporters, *Nature*, 2007, **446**, 749–757.
39 A. Ahmad, H. Varshney, A. Rauf, A. Sherwani and M. Owais, Synthesis and anticancer activity of long chain substituted 1, 3, 4-oxadiazol-2-thione, 1, 2, 4-triazol-3-thione and 1, 2, 4-triazolo [3, 4-b]-1, 3, 4-thiadiazine derivatives, *Arabian J. Chem.*, 2017, **10**, S3347–S3357.
40 B. Liu, C. Cui, W. Duan, M. Zhao, S. Peng, L. Wang, H. Liu and G. Cui, Synthesis and evaluation of anti-tumor activities of N4 fatty acyl amino acid derivatives of 1-β-arabinofuranosylcytosine, *Eur. J. Med. Chem.*, 2009, **44**, 3596–3600.
41 A. Kantankar, Y. J. Rao, G. Mallikarjun, Y. Hemasri and R. R. Kethiri, Rational design, synthesis, biological evaluation and molecular docking studies of chromone-pyrimidine derivatives as potent anti-cancer agents, *J. Mol. Struct.*, 2021, **1239**, 130502.
42 M. Sahlabadi, M. Daryanavard, H. Hadadzadeh and Z. Amirghofran, A nanocomplex of Cu (II) with theophylline drug; synthesis, characterization, and anticancer activity against K562 cell line, *J. Mol. Struct.*, 2018, **1155**, 450–456.